The Astrophysical Journal, 651: L117–L120, 2006 November 10

SPITZER MEASUREMENTS OF ATOMIC AND MOLECULAR ABUNDANCES IN THE TYPE IIP SN 2005af

Rubina Kotak,[1] Peter Meikle,[2] Monica Pozzo,[2] Schuyler D. van Dyk,[3] Duncan Farrah,[4] Robert Fesen,[5] Alexei V. Filippenko,[6] Ryan J. Foley,[6] Claes Fransson,[7] Christopher L. Gerardy,[2] Peter A. Höflich,[8] Peter Lundqvist,[7] Seppo Mattila,[9] Jesper Sollerman,[10] and J. Craig Wheeler[11]

Received 2006 August 30; accepted 2006 September 25; published 2006 October 23

ABSTRACT

We present results based on mid-infrared (3.6–30 μm) observations with the *Spitzer Space Telescope* of the nearby Type IIP supernova 2005af. We report the first ever detection of the SiO molecule in a Type IIP supernova. Together with the detection of the CO fundamental, this is an exciting finding as it may signal the onset of dust condensation in the ejecta. From a wealth of fine-structure lines we provide abundance estimates for stable Ni, Ar, and Ne that, via spectral synthesis, may be used to constrain nucleosynthesis models.

Subject headings: supernovae: general — supernovae: individual (SN 1987A, SN 2004dj, SN 2005af)

Online material: color figures

1. INTRODUCTION

Mid-infrared (mid-IR) studies of supernovae (SNe) have been hampered by a combination of several factors: their intrinsic faintness at epochs of interest, the high background at mid-IR wavelengths, and strong terrestrial atmospheric absorption. With the sole exception of the extremely nearby (50 kpc) SN 1987A (Roche et al. 1993; Wooden et al. 1993), this wavelength region has remained out of reach for SN studies. Yet, access to the mid-IR region is important for at least two reasons. First, a large number of fine-structure lines that are sensitive to the details of the explosion physics lie in the 5–40 μm region. These provide robust measurements of element abundances permitting direct comparisons with explosion models. Second, core-collapse SNe (CCSNe) have been proposed to be major sources of dust at high redshifts (e.g., Todini & Ferrara 2001), but even in the local universe, this hypothesis rests on little direct observational evidence. By monitoring the mid-IR evolution, where warm dust emits most strongly, we have a powerful means by which we can ascertain the epoch of dust condensation and estimate the amount of fresh dust produced in the ejecta. Alternatively, via mid-IR measurements, we can study the development of an IR echo arising in the preexisting dusty circumstellar medium, thereby constraining the presupernova evolution of the progenitor (e.g., Meikle et al. 2006).

The improvements in terms of sensitivity and spatial resolution afforded by the *Spitzer Space Telescope* finally allow us to probe SN behavior using mid-IR diagnostics. To this end, we are pursuing a multiepoch spectroscopic and photometric campaign of a significant sample of SNe of all types, within the framework of the Mid-IR Supernova Consortium. Fortuitously, since the launch of *Spitzer*, at least half a dozen CCSNe have exploded within ~10 Mpc. Recently, we presented a first mid-IR study of the nearest (3.13 Mpc) of these, SN 2004dj (Kotak et al. 2005). Here we describe results for the Type IIP SN 2005af that highlight the diversity of this subgroup.

SN 2005af was discovered in the nearby edge-on spiral galaxy, NGC 4945, on 2005 February 8.22 (UT) at $V = +12.8$ by Jacques & Pimentel (2005). On the basis of a spectrum obtained 4 days later, Filippenko & Foley (2005) classified it as a Type IIP (plateau) supernova, at an epoch of about 1 month post-explosion. In what follows, we assume that the supernova exploded on 2005 January 9, but note that the explosion epoch is probably uncertain by up to a few weeks. NGC 4945 is associated with the Centaurus group of galaxies, and estimates of its distance have ranged from 3.9 (de Vaucouleurs et al. 1981) to 8.1 Mpc (Baan 1985). In recent years, these values have tended to converge near the lower end of this range. Following the reasoning in Bergman et al. (1992 and references therein), we adopt a distance of 3.9 Mpc.

2. OBSERVATIONS

We first observed SN 2005af with *Spitzer* during Cycle 1 using the Infrared Spectrograph (IRS) and IRS Peak-up Imaging (PUI) under Director's Discretionary Time program 237. We subsequently observed it during Cycle 2 as part of our GO Program 20256, using the Infrared Array Camera (IRAC), IRS, and IRS PUI.

2.1. *Photometry*

The 3.6–8.0 μm imaging with IRAC was obtained on 2005 July 22 (194 days) and 2006 February 12 (399 days). A frame time of 30 s and five (medium-sized) dither positions in mapping mode for each pair of channels were used. Our measurements from aperture photometry, carried out on the post–Basic Calibrated Data (BCD), version S14.0.0 image mosaics using GAIA, are shown in Table 1. At 67 days, SN 2005af is very bright in all four IRAC channels, The flux is particularly bright in channel 2 (4.5 μm). Nevertheless, examination of individual

[1] ESO, Karl-Schwarzschild Strasse 2, Garching-bei-München, D-85748, Germany; rkotak@eso.org.
[2] Astrophysics Group, Imperial College London, Blackett Laboratory, Prince Consort Road, London SW7 2AZ, UK.
[3] *Spitzer* Science Center, 220-6, Pasadena, CA 91125.
[4] Department of Astronomy, Cornell University, 106 Space Sciences, Ithaca, NY 14853.
[5] Department of Physics and Astronomy, 6127 Wilder Laboratory, Dartmouth College, Hanover, NH 03755.
[6] Department of Astronomy, University of California, Berkeley, CA 94720-3411.
[7] Department of Astronomy, Stockholm University, AlbaNova, SE-10691 Stockholm, Sweden.
[8] Department of Physics, Florida State University, 315 Keen Building, Tallahassee, FL 32306-4350.
[9] Department of Physics and Astronomy, Queen's University Belfast, Belfast BT7 1NN, Northern Ireland.
[10] Dark Cosmology Centre, Niels Bohr Institute, University of Copenhagen, Juliane Maries Vej 30, 2100 Copenhagen Ø, Denmark.
[11] Astronomy Department, University of Texas at Austin, Austin, TX 78712.

TABLE 1
PHOTOMETRY OF SN 2005af

DATE	EPOCH (day)	t_{exp} (s)	FLUX (mJy) IRAC 3.6 μm	IRAC 4.5μm	IRAC 5.8 μm	IRAC 8.0 μm	PUI 16 μm
2005 Mar 17	67	1219	...	...	...	...	5.0 ± 0.3
2005 Jul 22	194	524	3.96 ± 0.02	17.54 ± 0.04	9.31 ± 0.05	7.43 ± 0.06	[3.10]
2005 Aug 08	211	629	...	...	...	...	2.83 ± 0.03
2006 Feb 12	399	524	0.93 ± 0.02	3.43 ± 0.02	2.24 ± 0.02	4.84 ± 0.07	[2.63]
2006 Mar 18	433	629	...	...	...	...	2.19 ± 0.03

NOTES.—Photometry was carried out using a 5.″5 radius aperture for all channels. This aperture was chosen to enclose the full diffraction pattern to the first dark ring at the PUI red limit of 18.7 μm. The aperture was positioned using WCS coordinates. Aperture corrections as appropriate for the outer diffraction rings were applied to IRAC channels 1–4 using Table 5.7 of the IRAC data handbook. No attempt was made to apply a color correction to the measured PUI fluxes, since the choice of temperature is not obvious. However, we note that the correction would be $\lesssim$2% for hot dust (500–1000 K), and that such a correction would lie well within our errors. We estimated the systematic error due to variations in the background by repeating our measurements with differing annuli. The errors above are a combination of systematic and statistical errors. The figures in square brackets under the PUI column are indications of the expected fluxes coeval with the IRAC values assuming a *Q*-band decline rate similar to that of SN 1987A. t_{exp} is the on-source integration time.

BCD frames showed that saturation had not occurred; i.e., the measurements are robust.

Our first epoch of PUI 16 μm imaging was obtained in Peak-Up mode only, i.e., before dithering capabilities were offered with IRS. The two subsequent epochs of PUI observations were carried out using 31.46 s ramps and 20 small-scale dither positions. The SN was clearly detected at all three epochs (Table 1).

2.2. *Spectroscopy*

Spectra were obtained on 2005 March 17 (67 days) and 2005 August 11 (214 days) with the Short-Low (SL, $\lambda = 5.2$–14.5 μm; $R = 64$–128) module of the IRS in staring mode. A Long-Low (LL, $\lambda = 14$–38 μm; $R = 64$–128) spectrum was also acquired at 67 days. For the SL mode, the total time on-source at the two epochs was 1219 and 1828.5 s, respectively, and 629 s for the LL mode.

The first- and second-epoch data were preprocessed using versions S12.3.0 and S12.4.0, respectively, of the *Spitzer* data processing pipeline. We began the reduction of the BCD data by differencing the two nod positions to remove the background emission. All subsequent steps, i.e., straightening, extraction, and wavelength and flux calibration, were carried out using SPICE version 1.1-beta15 with standard settings.

The spectra are shown in Figure 1. We also extracted the spectra using post-BCD S13.2.0 products and found that they were virtually identical.

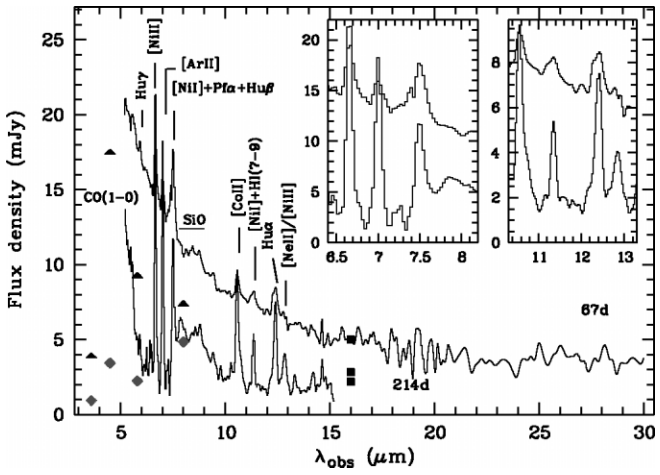

FIG. 1.—Mid-IR spectra of SN 2005af for days 67 (*top curve*) and 214 (*bottom curve*). Plausible line identifications are marked. The IRAC measurements are shown as triangles (194 days) and (*red*) diamonds (399 days), while the black squares show the PUI measurements for days 67, 211, and 433 from top to bottom, respectively. Note the sharp drop in flux between the two IRAC epochs at 4.5 μm, and the relative increase in prominence of the flux at $\sim$8 μm. The IRS flux levels are consistent with the photometry. The insets show the evolution of line profiles described in § 3. [*See the electronic edition of the Journal for a color version of this figure.*]

3. ANALYSIS

The high IRAC flux at 4.5 μm for the first epoch compared to other channels is almost certainly due to CO fundamental band emission. This is corroborated by the steep rise toward 5 μm in both spectra, which we identify with the red wing of the CO fundamental (see Fig. 1). Between 194 and 399 days, the sharpest decline in IRAC flux is seen at 4.5 μm. These observations suggest that CO formed in the ejecta less than 2 months after explosion, persisting to at least 7 months, but had faded substantially by about 1 year. The relative increase in the IRAC channel 4 (8 μm) flux by 399 days is probably due to the emergence of spectral features in the 6.43–9.40 μm region spanned by this channel. This is discussed below.

By day 214, a pedestal-like feature appears spanning $\sim$7.6–9 μm, which we identify with molecular emission due to the SiO fundamental band (Figs. 1 and 3). This is the first time that SiO has been detected in the ejecta of a SN IIP—the most common subtype of all CCSNe at low redshifts. The only other detection of SiO in SN ejecta was in the peculiar Type II SN 1987A (Roche et al. 1991; Wooden et al. 1993). That molecules are detected at all provides a diagnostic of the prevalent conditions in the ejecta. As both CO and SiO are powerful coolants, they are regarded as precursors to dust condensation in the ejecta (e.g., Nozawa et al. 2003).

In Figure 2 we compare an LTE model SiO spectrum for SN 1987A at 260 days (Liu & Dalgarno 1994) with the day 214 SL spectrum of SN 2005af. The model, attenuated by a factor of 2.5, produces a convincing reproduction of the observed behavior. Scaling from the model, the match to our spectrum suggests a SiO mass of $\sim 2 \times 10^{-4}\ M_{\odot}$. Liu & Dalgarno (1994, 1996) argue that such a mass can only form if there is no mixing of helium into the oxygen-silicon region of the ejecta.

Apart from molecular emission, several conspicuous lines are visible in both spectra (Fig. 1) that were identified by analogy

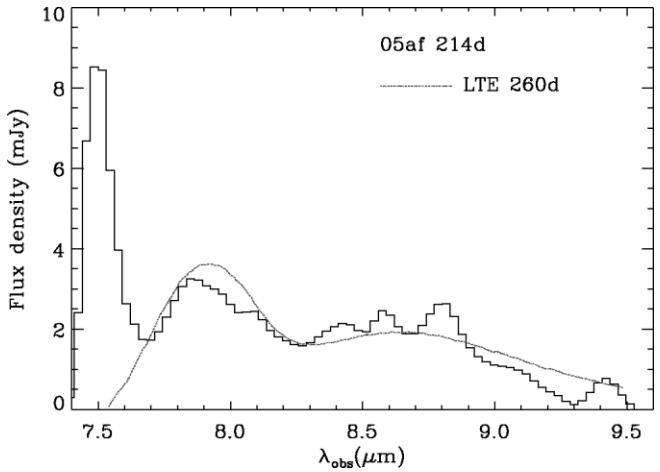

FIG. 2.—The 260 day LTE model from Liu & Dalgarno (1994) attenuated by a factor of 2.5, superposed on the continuum-subtracted second-epoch spectrum of SN 2005af. From this, we deduce a SiO mass of $\sim 2 \times 10^{-4}$ $M_\odot$ (§ 3). [*See the electronic edition of the Journal for a color version of this figure.*]

with SN 1987A (Wooden et al. 1993). At both epochs, the spectrum is dominated by forbidden lines of Ni, Co, and Ar, of which the [Ni II] 6.64 μm, [Ar II] 6.99 μm, and [Co II] 10.52 μm are the most prominent.

Between 67 and 214 days the lines show appreciable increases in intensity (see Table 2, Fig. 1). In addition, in spite of the low spectral resolution ($R = 64$–128), we observe in a number of lines (e.g., [Ni II] 6.64 μm, [Co II] 10.52 μm) an extended red wing at 67 days that fades by 214 days. The broad blend with an extended red wing near 11.3 μm at 67 days is probably due to a combination of [Ni I] and H I (7–9), but by 214 days, it is symmetric.

Extended red wings were also detected in several lines in SN 1987A (e.g., Witteborn et al. 1989), accompanied by small redshifts of the line centroid. A plausible explanation is provided by electron scattering in the expanding hydrogen envelope (Fransson & Chevalier 1989). This may also apply to SN 2005af, although we do not detect any obvious redshifting of line centroids.

We now estimate the abundances from the stronger lines at the later epoch when the ejecta has a lower optical depth. Following McCray (1990) we estimate the electron density of the ejecta as $n_e \sim 10^8 t_{\rm yr}^{-3.5}$ cm$^{-3} \approx 7 \times 10^8$ cm^{-3} at day 214. We derived critical densities for Ni^+ and Ar^+ using collision strengths from Bautista & Pradhan (1996) and Osterbrock & Ferland (2006), respectively, and found these to be 1–3 orders of magnitude smaller than n_e. On this basis, we deem an LTE treatment to be valid.

Using the line intensities in Table 2, we derive masses using the upper excited state populations of the ions and find 3.7×10^{-3}, 1×10^{-3}, and 2.2×10^{-3} $M_\odot$ for stable (Ni^0, Ni^+), Ar^+, and Ne^+, respectively, for an electron temperature of 4000 K. Note that the result is insensitive to temperature: a ± 1000 K change in temperature changes the mass estimates by $\lesssim$15%. The partition functions are from Halenka et al. (2001) for Ni, and Irwin (1981) for Ar and Ne. Assuming a uniform distribution of stable Ni, we find that the Sobolev optical depths of all detected Ni lines are less than 0.06. Strong transitions of [Ni III] 11.002 μm and [Ni IV] 8.405 μm lie within the wavelength region covered, but these lines are not detected at either epoch. We conclude that the Ni is predominantly in the neutral and singly ionized state. Thus, assuming insignificant clumping, the value we derive above is probably close to the total stable Ni mass.

TABLE 2
LINE INTENSITIES

λ_{rest} (μm)	Ion	Instrum. Res. (km s^{-1})	67 days I	67 days FWHM (km s^{-1})	214 days I	214 days FWHM (km s^{-1})
6.636	[Ni II]	2700	3.18	4000	9.42	3600
6.985	[Ar II]	2600	1.61	3800	6.16	3000
7.507	[Ni I]	2400	…	…	4.48	4000
10.521[a]	[Co II]	3400	0.78	4500	1.99	3000
11.308[b]	[Ni I]	3200	0.25	2400	0.78	2900
12.813[c]	[Ne II]	2800	…	…	0.56	3300

NOTES.—The intensities were measured after subtracting a continuum fitted by a low-order polynomial or a spline function; the FWHM were derived from Gaussian fits. The third column lists the instrumental resolution; I, the intensity, is in units of 10^{-14} ergs cm^{-2} s^{-1}.

[a] As this line is symmetric, we assumed that there was no blend with [Ni II] 10.68 μm.

[b] At 67 days this line has a probable contribution from H I(7–9) but by day 214, it is symmetric; above, we assume that it arises due to [Ni I] only. Interestingly, the H I(7–9) feature was not detected in SN 1987A at 60 days (Wooden et al. 1993).

[c] The 12.8 μm feature at 214 days is likely to be a blend of [Ne II] λ12.813 μm and [Ni II] λ 12.729 μm. Given the strength of the [Ni II] 6.636 μm line, we estimate that the 12.8 μm blend comprises roughly equal contributions from the two elements. At 67 days, however, given the strength of the [Ni II] 6.636 μm line, the [Ni II] 12.729 μm line would have been barely detectable.

The predicted mass of stable Ni is sensitive to the progenitor mass, although this relation is not monotonic, and depends sensitively on the explosion mechanism, multidimensional effects and, in spherical models, on the mass cut, which is a free parameter. Thielemann et al. (1996) predict stable Ni masses in the range 0.01–0.014 $M_\odot$ for progenitors in the range 13–20 $M_\odot$, and a much lower value of 0.002 $M_\odot$ for a 25 $M_\odot$ star. Other authors (e.g., Chieffi & Limongi 2004; Woosley & Weaver 1995; Nomoto et al. 2006) derive comparable values, although detailed intercomparisons are difficult due to different parameterizations of physical processes.

Chieffi & Limongi (2004) provide explosive yields as a function of metallicity based on parameters which have been calibrated to fit observed properties of massive stars. The value for the stable Ni mass that we derive is closest to their progenitor models of 13–15 $M_\odot$ with metallicities of a third to a twentieth of the solar value. Although we can definitively rule out higher mass progenitors at even lower metallicities, we current cannot exclude a 35 $M_\odot$ progenitor at solar metallicity. Further, planned, late-time spectroscopy should provide tighter constraints.

Given the high energy required to ionize neutral Ne (21.6 eV) and Ar (15.8 eV), we conclude that, given the low-ionization conditions indicated by Ni, the bulk of the Ne and Ar lies in the neutral state. However, no strong transitions of [Ne I] or [Ar I] lie in our wavelength range. Consequently, the masses derived here for the first ionization state represent lower limits only.

For SN 1987A at 260 days, using the [Co II] 10.52 μm line, Roche et al. (1993) derive a value for $M_{\rm Co^+}$ of 4.6×10^{-3} $M_\odot$. Using our day 214 intensity for this line in SN 2005af, we obtain $M_{\rm Co^+} = 2.4 \times 10^{-3}$ $M_\odot$. Allowing for the different epochs for the two SNe, this implies that a ^{56}Ni mass of 0.027 $M_\odot$ was ejected by SN 2005af. This estimate falls in the expected range for normal Type II SNe (e.g., Hamuy 2003).

Although we have a clear detection of the SN 2005af spec-

trum between 16 and 30 μm (Fig. 1)—the first, for any SN at this early epoch—we do not see any significant spectral features. This is not surprising, given its youth. In SN 1987A, lines of [Fe II] in this spectral region were only detected after ~400 days (Haas et al. 1990).

3.1. *Comparison with Other Type II SNe*

In Figure 3 we compare roughly coeval mid-IR spectra of SN 2005af with that of SN 1987A (IIpec) at ~60 days, and with those of SN 1987A and SN 2004dj (IIP) at ~250 days. The 60 day mid-IR spectrum of SN 1987A is dominated by H I lines (see Fig. 3 or Roche et al. 1993; Wooden et al. 1993). In contrast, strong lines of [Ni II] and [Ar II] are present in SN 2005af. This suggests either that our first-epoch SN 2005af observations were taken on the radioactive tail of the light curve and that the length of the plateau phase must have been $\lesssim$60 days, or that the estimated explosion date, based on the classification spectrum, is too late by $\gtrsim$1 month.

At the later epoch all three SNe exhibit prominent lines of nickel and cobalt. Wooden et al. (1993) emphasize that the ratio of [Ni I] 7.5 μm to [Ni II] 6.64 μm lines provides a sensitive measure of the ionization fraction of Ni ($\chi_{\rm Ni} = n_{\rm Ni^+}/n_{\rm Ni}$). Using their Fig. 9, and assuming LTE, we find $\chi_{\rm Ni} \approx 0.35$,0.55, and 0.85 for SN 2004dj, SN 2005af, and SN 1987A, respectively, at ~250 days.

SN 2005af shows much stronger [Ar II] than SN 1987A. Moreover, SN 2004dj is found to be a factor of 20 weaker than SN 2005af in this line. Even if we normalize to the strengths of the adjacent [Ni II] 6.63 μm, [Ni I] 7.50 μm lines, the [Ar II] line is still over 5 times stronger in SN 2005af. This is intriguing given that SNe 2004dj and 2005af are both of Type IIP. One possibility, indirectly implied by $\chi_{\rm Ni}$ above, is that the conditions required to ionize Ar are not attained in SN 2004dj, while Ni^+, with its lower ionization potential (7.6 eV), is easier to produce.

Another hint may come from the spherically symmetric Thielemann et al. (1996) models, where the bulk of the stable Ar (mostly ^{36}Ar) is formed in a shell just above the stable Ni region. Thus, one might expect that a higher mass cut (below which the core collapses to a neutron star or black hole) within the Ni zone would produce a lower absolute Ni mass, but a higher Ar/Ni mass ratio. However, this seems to be contrary to what we observe; i.e., SN 2004dj has an apparently smaller Ni mass but an even smaller Ar/Ni mass ratio than SN 2005af. We suspect that to account for this behavior, a certain degree of asymmetry or clumpiness, as well as mixing in the ejecta, has to be invoked. Interestingly, Pereyra et al. (2006) infer an overall asphericity of 20% for SN 2005af from optical polarimetry.

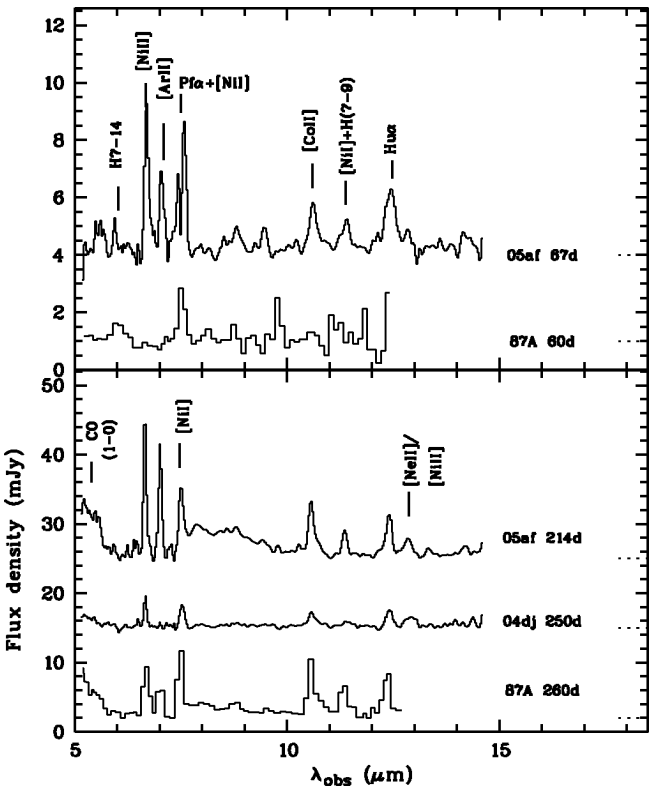

FIG. 3.—Comparison of continuum-subtracted spectra of CCSNe at roughly coeval epochs. The dotted lines mark the zero-level. Note the striking difference in the strength of the [Ar II] line at ~200 days between the SNe. The SN 1987A spectra are from Wooden et al. (1993); the 260 day spectrum has been divided by a factor of 5. Isolated features that are common to both epochs are labeled in the top panel only; features that are evident in the later epoch only are indicated in the lower panel. The SN 2004dj spectrum is part of our ongoing monitoring program; a fuller analysis of these data will be presented elsewhere.

This work is based on observations made with the *Spitzer Space Telescope*, which is operated by the Jet Propulsion Laboratory, California Institute of Technology under NASA contract 1407. Financial support for the research is provided by NASA/*Spitzer* grant GO-20256. Support for this work was provided by NASA through an award issued by JPL/Caltech. R. K. and S. M. acknowledge support from an ESO fellowship and from the EURYI Awards scheme, respectively.

REFERENCES

Baan, W. A. 1985, Nature, 315, 26
Bautista, M. A., & Pradhan, A. K. 1996, A&AS, 115, 551
Bergman, P., et al. 1992, A&A, 265, 403
Chieffi, A., & Limongi, M. 2004, ApJ, 608, 405
de Vaucouleurs, G., et al. 1981, ApJ, 248, 408
Fransson, C., & Chevalier, R. A. 1989, ApJ, 343, 323
Filippenko, A. V., & Foley, R. J. 2005, IAU Circ. 8484
Haas, M. R., et al. 1990, ApJ, 360, 257
Halenka, J., et al. 2001, Acta Astron., 51, 347
Hamuy, M. 2003, ApJ, 582, 905
Irwin, A. W. 1981, ApJS, 45, 621
Jacques, C., & Pimentel, E. 2005, IAU Circ. 8482
Kotak, R., et al. 2005, ApJ, 628, L123
Liu, W., & Dalgarno, A. 1994, ApJ, 428, 769
———. 1996, ApJ, 471, 480
Meikle, W. P. S., et al. 2006, ApJ, in press (astro-ph/0605584)
McCray, R. 1990, Molecular Astrophysics (Cambridge: Cambridge Univ. Press)
Nomoto, K., et al. 2006, preprint (astro-ph/0605725)
Nozawa, T., et al. 2003, ApJ, 598, 785
Osterbrock, D. E., & Ferland, G. 2006, Astrophysics of Gaseous Nebulae and Active Galactic Nuclei (Mill Valley: University Science Books)
Pereyra, A., et al. 2006, A&A, 454, 827
Roche, P., Aitken, D., & Smith, C. 1991, MNRAS, 252, 39P
———. 1993, MNRAS, 261, 522
Thielemann, F.-K., et al. 1996, ApJ, 460, 408
Todini, P., & Ferrara, A. 2001, MNRAS, 325, 726
Witteborn, F. C., et al. 1989, ApJ, 338, L9
Wooden, D., et al. 1993, ApJS, 88, 477
Woosley, S. E., & Weaver, T. A. 1995, ApJS, 101, 181